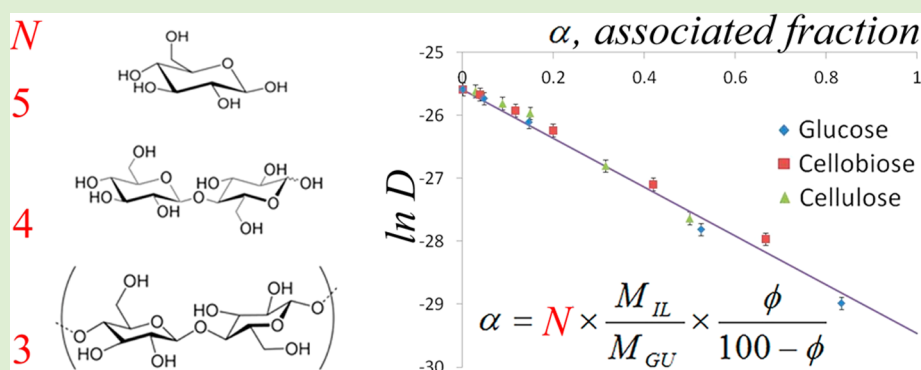


# Diffusion of 1-Ethyl-3-methyl-imidazolium Acetate in Glucose, Cellobiose, and Cellulose Solutions

Michael E. Ries,<sup>\*,†</sup> Asanah Radhi,<sup>†</sup> Alice S. Keating,<sup>†</sup> Owen Parker,<sup>†</sup> and Tatiana Budtova<sup>‡</sup>

<sup>†</sup>Soft Matter Physics Research Group, School of Physics and Astronomy, University of Leeds, Leeds, LS2 9JT, United Kingdom

<sup>‡</sup>Mines ParisTech, Centre de Mise en Forme des Matériaux (CEMEF), UMR CNRS 7635, BP 207, 06904 Sophia Antipolis, France



**ABSTRACT:** Solutions of glucose, cellobiose and microcrystalline cellulose in the ionic liquid 1-ethyl-3-methyl-imidazolium ([C2mim][OAc]) have been examined using pulsed-field gradient  $^1\text{H}$  NMR. Diffusion coefficients of the cation and anion across the temperature range 20–70 °C have been determined for a range of concentrations (0–15% w/w) of each carbohydrate in [C2mim][OAc]. These systems behave as an “ideal mixture” of free ions and ions that are associated with the carbohydrate molecules. The molar ratio of carbohydrate OH groups to ionic liquid molecules,  $\alpha$ , is the key parameter in determining the diffusion coefficients of the ions. Master curves for the diffusion coefficients of cation, anion and their activation energies are generated upon which all our data collapses when plotted against  $\alpha$ . Diffusion coefficients are found to follow an Arrhenius type behavior and the difference in translational activation energy between free and associated ions is determined to be  $9.3 \pm 0.9$  kJ/mol.

## INTRODUCTION

Biomass-based polymers are taking a more and more important place in the development of sustainable and “green” cost-effective industry.<sup>1</sup> Cellulose is the most abundant naturally occurring biopolymer and is a practically inexhaustible resource for the production of environmentally friendly, biodegradable, and biocompatible products.<sup>2</sup> It is also a source of numerous derivatives, cellulose ethers, and esters. Despite these advantages, the full potential of cellulose has not yet been realized. The main challenge until now has been a lack of nonderivatizing, nontoxic, and easy to handle solvents for cellulose dissolution. Strong inter- and intramolecular hydrogen bonds in cellulose hinder it from being easily dissolved in common polymer solvents.<sup>3,4</sup>

In 1914, Walden published work on synthesizing ethylammonium nitrate, which is often described as the first intentionally developed room-temperature ionic liquid.<sup>5</sup> The term ionic liquid (IL) has now come to mean a salt that, due to its poorly coordinating ions, is in the liquid state below 100 °C.<sup>6</sup> There has been a great deal of interest in ILs because of their ability to act as versatile solvents, particularly for some difficult to dissolve polysaccharides such as cellulose, with it being demonstrated<sup>7</sup> that solvent systems containing the IL

[C4mim]Cl are capable of partially dissolving untreated wood. ILs are now also suggested for biomass pretreatment, fractionation, and making monomeric sugars for biofuel production.<sup>8,9</sup> All this combined with some of their other properties, negligible vapor pressure, high thermal stability, and nonflammability, have made them very desirable for use in industry as “green” solvents. Furthermore, ILs have highly tunable properties<sup>7,10,11</sup> through the variety of cation and anion chemical structures and combinations, which enable viscosity, solubility, density, ionic conductivity, and melting point to be altered.

It was found<sup>3</sup> that without cellulose pretreatment, certain ILs, mainly based on imidazolium or pyridinium cations and chloride and acetate anions, have the ability to dissolve up to 20% w/w of cellulose. Fibres,<sup>12</sup> films<sup>13</sup> and aerogels<sup>14</sup> have been prepared from cellulose-IL solutions. ILs are also being used as reaction media for the homogeneous synthesis of cellulose derivatives.<sup>15</sup> In order to advance toward use and optimization of ILs as cellulose solvents, a comprehensive

Received: November 8, 2013

Revised: December 18, 2013

Published: January 9, 2014

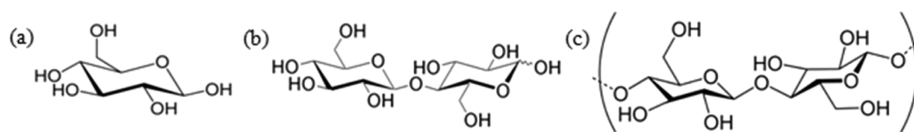


**Figure 1.** Chemical structure of (a) glucose, (b) cellobiose, and (c) cellulose.

understanding of the mechanisms of cellulose dissolution and of IL interactions with the solute is extremely important.

Cellulose dissolution in ionic liquids probed by NMR,<sup>16,17</sup> molecular modeling<sup>18</sup> of carbohydrate-IL interactions and the properties of cellulose-IL solutions<sup>19–22</sup> have been extensively studied during the past decade. To help understand the mechanisms of cellulose dissolution in ILs, glucose,<sup>23,24</sup> and cellobiose<sup>17,23</sup> have also been used as they are the building blocks of cellulose. Most experimental and modeling results show that ILs solvate carbohydrates through the formation of hydrogen bonds between the IL anion and hydroxyl groups of the sugar solutes.<sup>16,18,24,25</sup>

Some authors suggest, however, that the heterocyclic cation plays an important role in that it “prefers to associate with oxygen atoms of hydroxyls”.<sup>17</sup> Following 1-butyl-3-methylimidazolium chloride anion and cation relaxation times in solutions of glucose and cellobiose it was suggested that chloride ions interact in a 1:1 ratio with carbohydrate hydroxyl protons.<sup>16</sup> A similar ratio of 1-ethyl-3-methylimidazolium ([C2mim][OAc]) to hydroxyl between 3:4 and 1:1 was reported in NMR spectroscopic studies of cellobiose solvation in [C2mim][OAc].<sup>17</sup>

The goal of this work is to clarify and quantify the interactions between the imidazolium based ionic liquid [C2mim][OAc] and carbohydrates by a detailed and extended NMR comparative study of cellulose, cellobiose, and glucose dissolved in [C2mim][OAc]. The diffusion coefficients of the ions in cellobiose and glucose solutions in the concentration range of 0–15% w/w of carbohydrate have been measured over the range of temperatures 20–70 °C. These results were analyzed together with [C2mim][OAc] diffusion coefficients in cellulose solutions in the same range of carbohydrate concentrations and solution temperatures, obtained in our previous work.<sup>22</sup> We demonstrate that the amount of OH groups on each anhydroglucose unit, that is, 5 on glucose, 4 on cellobiose, and 3 on cellulose, is the key parameter describing carbohydrate dissolution in this ionic liquid. We confirm this hypothesis by the analysis of changes in the position of chemical shifts upon addition of each carbohydrate.

## EXPERIMENTAL SECTION

**Materials and Sample Preparation.** Glucose and cellobiose were purchased from Sigma Aldrich and prior to dissolution these materials were dried under vacuum at 80 °C for a period of 12 h. In Figure 1 the structures of glucose, cellobiose and cellulose are shown. The ionic liquid 1-ethyl-3-methylimidazolium [C2mim][OAc] (97% purity) was purchased from Sigma Aldrich and used without further purification. Neat [C2mim][OAc] and two sets of samples (glucose/cellobiose) each with five concentrations of the corresponding carbohydrate (1, 3, 5, 10, and 15% w/w) in [C2mim][OAc] were prepared. Diffusion data from our previous publication<sup>22</sup> on [C2mim][OAc] with microcrystalline cellulose Avicel PH-101 with degree of polymerization 180 (cellulose in the following) purchased from Sigma Aldrich is also included in this work.

All the sample preparations were made in an MBraun Labmaster 130 atmospheric chamber under nitrogen, providing a dry environment, with the chamber being maintained at a dew point level between

–70 and –40 °C. The [C2mim][OAc] and glucose/cellobiose/cellulose were mixed and stirred in a small container at 70 °C for a minimum of 48 h. A small quantity of each carbohydrate [C2mim][OAc] solution was then placed in a standard 5 mm NMR tube within the chamber. Each tube was sealed still within the chamber to prevent moisture contamination. When the samples were not in use they were stored in a desiccator.

**Pulsed-Field Gradient <sup>1</sup>H NMR Spectroscopy.** Diffusion coefficients of both the cation [C2mim]<sup>+</sup> and anion [OAc]<sup>–</sup> were determined by a pulsed-field gradient <sup>1</sup>H NMR technique using a widebore Avance II NMR Spectrometer (Bruker Biospin) operating at a <sup>1</sup>H resonant frequency of 400 MHz. A Diff60 diffusion probe (Bruker Biospin) capable of producing a maximum field gradient of 24 T m<sup>–1</sup> was used in the experiments. The calibration of the gradient field strength was performed by measuring the self-diffusion coefficient of water at 20.0 ± 0.1 °C, which has the value (2.03 ± 0.01) × 10<sup>–9</sup> m<sup>2</sup> s<sup>–1</sup>. A subsequent check of the sample environment temperature was performed by measuring the temperature dependence of the diffusion coefficient of water with reference to results published by Holz et al.<sup>26</sup> The recommendations set out by Annat et al. were followed,<sup>27</sup> such as keeping sample depths to less than 1 cm to minimize convection currents on heating in the NMR spectrometer. We estimate the uncertainty in our diffusion coefficient values to be approximately 3%. Remsing et al. have previously published diffusion data for the 5% and 10% of both glucose and cellobiose in [C2mim][OAc] solutions and our data agree with their work within experimental uncertainties.<sup>23</sup>

In this study we used a stimulated echo pulse sequence with bipolar gradients. The attenuation of the signal intensity in this pulsed field gradient NMR experiment follows:<sup>28</sup>

$$\ln(S_i/S_{i0}) = -D_i \gamma^2 g^2 \delta^2 (\Delta - \delta/3 - \tau/2) \quad (1)$$

where  $S_i$  is the measured signal intensity of species  $i$  and  $D_i$  is the diffusion coefficient of that species,  $S_{i0}$  defines the initial signal intensity,  $\gamma$  is the proton gyromagnetic ratio,  $\delta$  is the pulse duration of a combined pair of bipolar pulses,  $\tau$  is the period between bipolar gradients,  $\Delta$  is the period separating the beginning of each pulse-pair (i.e., diffusion time), and  $g$  is the gradient strength. In each experiment the strength of the gradient pulse was incremented, while  $\delta$  (2–5 ms) and  $\Delta$  (60 ms) remained constant.  $\tau$  was kept constant at 2 ms. The 90° pulse width was 6.6 μs,  $g$  had maximum values between 200 and 600 G/cm, the number of scans was 16, and the repetition time was 6 s. The  $T_1$  relaxation times for the various resonances ranged from 600 to 1200 ms and  $T_2$  ranged from 100 to 400 ms. Our samples were studied in steps of 10 °C over the temperature range 20–70 °C inclusive. The signal intensities from the carbohydrate molecules were too small to follow reliably, so in this work we only report the values of the diffusion coefficients from the cation and anion of the ionic liquid.

## RESULTS AND DISCUSSION

**Diffusion of Ions in Glucose, Cellobiose, and Cellulose Solutions.** Across all temperatures and samples, each proton resonance only showed evidence of one diffusion coefficient, that is, each signal displayed simple linear dependences of the natural logarithm of the signal intensity  $S_i$  on the square of the gradient field strength  $g$ , recall eq 1. This indicates that if ion pairs/aggregates are forming, then the exchange between the free ions and the ion pairs/aggregates must be very fast (<ms). The same had already been reported for [C2mim][OAc] in cellulose-[C2mim][OAc] solutions.<sup>22</sup> Supporting this, each proton resonance has just one peak in each of the NMR

spectra, again confirming either the lack of ion pairs or the fast exchange between them and free ions. All the cation proton resonances for any given measurement were found to have the same diffusion coefficient within experimental uncertainty, as expected, since they are attached to the same diffusing ion. Therefore, only one average value will be used for the diffusion coefficient of cation  $D_{\text{cat}}$ . As for the anion, there is only one proton resonance with which its diffusion coefficient  $D_{\text{an}}$  was calculated.

In Figure 2 the cation diffusion coefficient  $D_{\text{cat}}$  is plotted against glucose (Figure 2a) and cellobiose (Figure 2b) weight fractions at various temperatures. Temperature increases

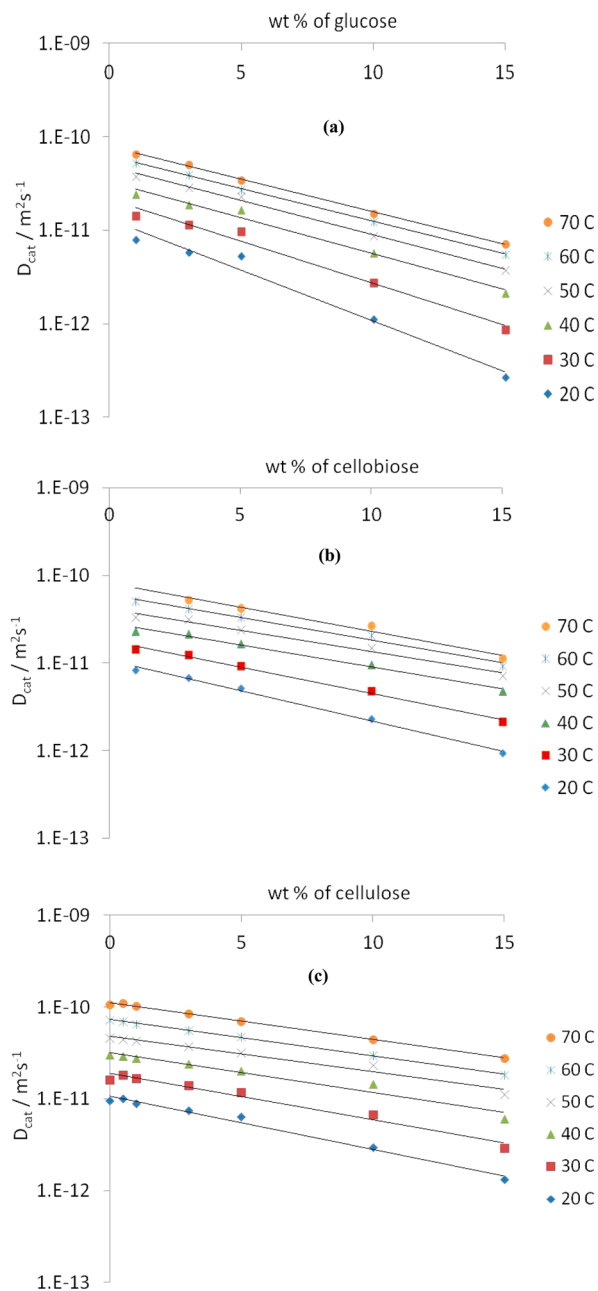


**Figure 2.** Diffusion coefficient of the cation ( $D_{\text{cat}}$ ) as a function of glucose (a), cellobiose (b), and cellulose (c) concentration. Straight lines indicate the best fit of exponential dependencies of  $D_{\text{cat}}$  on concentration. The cellulose data is taken from ref 22. The uncertainty in these values is approximately the size of the data points shown.

diffusion and the addition of carbohydrate decreases it. For completeness we show the results from our previous work<sup>22</sup> for [C2mim][OAc]-cellulose in Figure 2c.

An examination of Figure 2 shows that at a given temperature and carbohydrate concentration the cation diffusion varies in the following order: glucose < cellobiose < cellulose. This result is at first surprising in that the cellulose solutions have by far the highest viscosities and therefore from the point of view of the Stokes–Einstein relationship would be expected to have the slowest motion of ions, that is, the smallest ion diffusion coefficients. This reveals that the macroscopic zero shear rate viscosities combined with the Stokes–Einstein equation would not correctly predict the values of the cation diffusion coefficients. The effective local microviscosity experienced by the cations is instead the largest in the glucose solutions resulting in the smallest values for the diffusion coefficients.

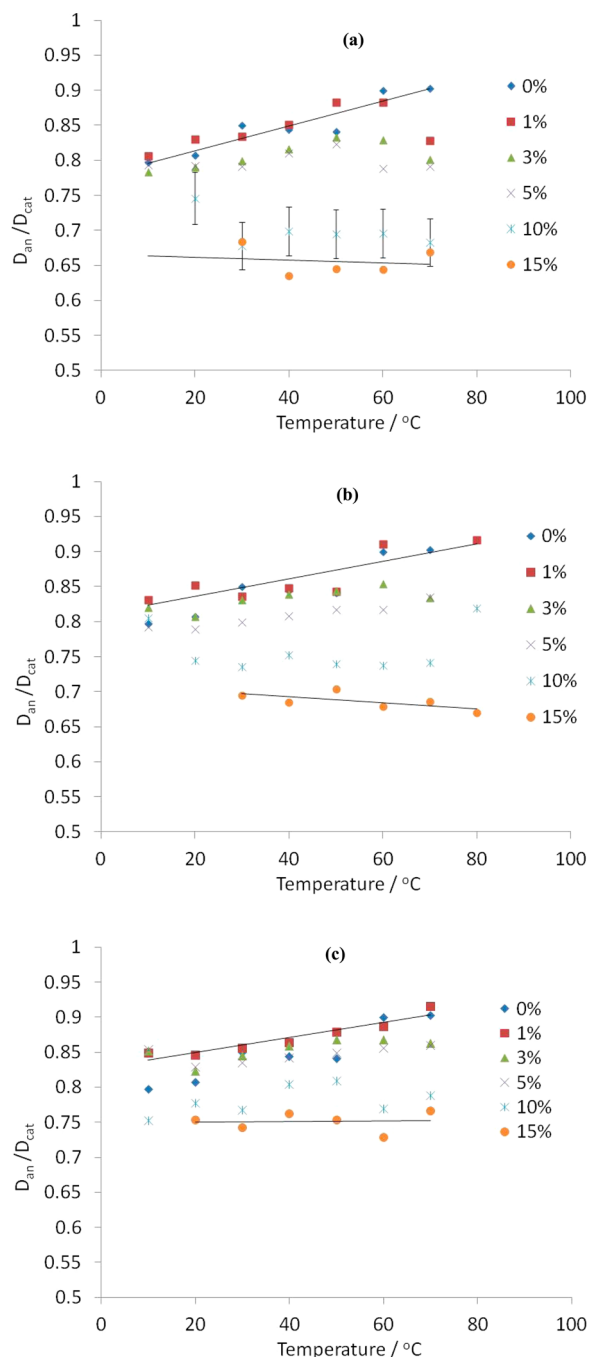
In earlier works on ionic liquids it was shown that the anion has a smaller diffusion coefficient than the cation ( $D_{\text{an}}/D_{\text{cat}} < 1$ ), with this being termed “anomalous” diffusion,<sup>29</sup> since the anion is geometrically smaller than the cation and therefore is expected to diffuse more quickly. It has been observed at higher temperatures and upon dilution<sup>10</sup> by a neutral solvent that the diffusion of both the cation and the anion species generally tend toward the value set by the inverse of the ratio of their hydrodynamic radii.<sup>30–33</sup> As shown in our earlier work<sup>22</sup> for cellulose-[C2mim][OAc] solutions, the effect of temperature on  $D_{\text{an}}/D_{\text{cat}}$  becomes weaker as the cellulose concentration becomes higher.

Figure 3a shows the ratio of the anion to cation diffusion coefficients for the glucose solutions, with this showing very similar trends to that already observed<sup>22</sup> for cellulose-[C2mim][OAc] solutions. It can be seen that the temperature dependence of this ratio is weakened by the addition of glucose. Furthermore, the increase of glucose concentration causes the diffusion to become more anomalous, that is, the anion diffuses yet slower relatively to the cation, further lowering the value of  $D_{\text{an}}/D_{\text{cat}}$ . This is consistent with the idea that the anion is more directly involved in the dissolution of the carbohydrate and therefore is more affected by its presence than the cation. These same temperature and concentration trends are seen for the cellobiose solutions, see Figure 3b. For completeness we show the ratio of  $D_{\text{an}}/D_{\text{cat}}$  for the cellulose samples (data taken from our earlier work<sup>22</sup>), see Figure 3c.

An important point to note from Figure 3 is that in terms of reducing the ratio of anion to cation diffusivities the glucose molecule is the most effective and cellulose the least. To illustrate this, consider the 40 °C data in Figure 3. For the pure IL, the ratio of  $D_{\text{an}}/D_{\text{cat}}$  is 0.85. This value decreases to 0.75 for the 15% cellulose, 0.7 for the 15% cellobiose, and 0.65 for the 15% glucose solutions.

Summarizing the results presented in Figures 2 and 3, we demonstrated that the glucose molecule is the most efficient at slowing down the ion diffusion in these carbohydrate solutions and that it preferentially slows down the anion relative to the cation. It is interesting therefore to compare the effect of the different carbohydrates on the ions’ diffusion coefficients directly, see an example for 20 °C in Figure 4.

In Figure 4a it can clearly be seen that at a given carbohydrate concentration the anion diffusion coefficient varies in the following order: glucose < cellobiose < cellulose. Also, it is useful to note at this point that the data are not linear in these semilog plots. The data in Figure 4a is for 20 °C, but



**Figure 3.** Ratio of anion diffusion coefficient to that of the cation,  $D_{an}/D_{cat}$  as a function of temperature for each concentration of glucose (a), cellobiose (b), and cellulose (c) given in weight percentage. The cellulose data are taken from our earlier work.<sup>22</sup> The size of the uncertainties is shown for the glucose 10% (w/w) data and each series has a similar sized uncertainty which have been left off the figure for clarity. Lines are given to guide the eye.

similar results are found for all temperatures measured. Furthermore, a very similar behavior is seen for the cation, see Figure 4b, despite it being less affected by the presence of the carbohydrate, recall Figure 3.

Now we put forward a hypothesis to explain the order of ionic liquid diffusion coefficients in these carbohydrate solutions, namely, glucose < cellobiose < cellulose. We suggest that it is the number of OH groups per mass of solute in these systems that determines how much the ions' diffusion

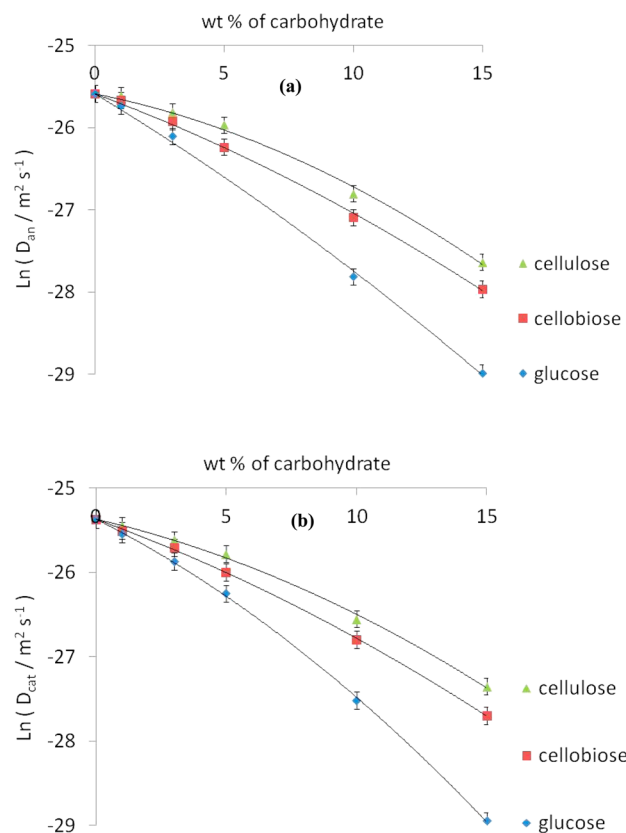


**Figure 4.** Diffusion coefficient of the anion  $D_{an}$  (a) and cation  $D_{cat}$  (b) at 20 °C as a function of carbohydrate weight percentage. The solid lines are simply guides to eye.

coefficients are reduced from their pure ionic liquid state. In Figure 1, the structure of glucose, cellobiose, and cellulose are shown. Cellulose consists of D-anhydroglucopyranose units (AGU) linked together by  $\beta(1\rightarrow4)$  glycosidic bonds. Each AGU unit within cellulose has three hydroxyl groups. Cellobiose is a disaccharide consisting of two D-glucopyranoses linked by a  $\beta(1\rightarrow4)$  bond. Each D-glucopyranose in cellobiose has four hydroxyl groups. Glucose is a monosaccharide with five hydroxyl groups. Therefore, instead of considering the data in terms of weight fraction of carbohydrate it is more useful to employ a molar ratio  $\alpha$  corresponding to the number of OH groups from the “glucose units” (D-anhydroglucopyranose/D-glucopyranose/D-glucose unit) per [C2mim][OAc] molecule, given by

$$\alpha = N \times \frac{M_{IL}}{M_{GU}} \times \frac{\phi}{100 - \phi} \quad (2)$$

where  $N$  is the number of OH groups per “glucose unit” (5, 4, and 3, respectively, for glucose, cellobiose, and cellulose),  $M_{IL}$  is the molar mass of the ionic liquid (170 g/mol),  $M_{GU}$  is the molar mass of a “glucose unit” (180, 171, and 162 g/mol, respectively, for glucose, cellobiose, and cellulose), and  $\phi$  the weight percent of the carbohydrate. We argue that the molar ratio  $\alpha$  is the fraction of IL molecules involved in dissolving all the “glucose units” for a given weight percentage of the carbohydrate and therefore can be considered as an associated fraction of the ionic liquid. It is important to note that in this analysis we are treating each OH from the carbohydrates as equally effective in reducing the value for the diffusion coefficients of the ions. A similar approach can be found in

the paper by Remsing et al.,<sup>16</sup> where they examined the NMR line widths in terms of bound and free fractions for the 1-*n*-butyl-3-methylimidazolium chloride carbohydrate (cellobiose/glucose) solutions. In their work<sup>16</sup> they found an almost 1:1 ratio of chloride ions to carbohydrate hydroxyl groups, having an  $N$  of 3.9 and 4.9 for cellobiose and glucose, respectively. It is also worth mentioning that Wang et al. showed<sup>1</sup> in their analysis of a wide selection of ILs that the molar ratio of IL to OH was  $2.1 \pm 0.3$  at the cellulose solubility limit for each IL, showing the fundamental importance of this ratio in carbohydrate dissolution.

To see if  $\alpha$  is the appropriate parameter to quantify the effect of the carbohydrate on the diffusion properties of the ions, we plot the diffusion coefficients of the ions against  $\alpha$  in Figure 5.

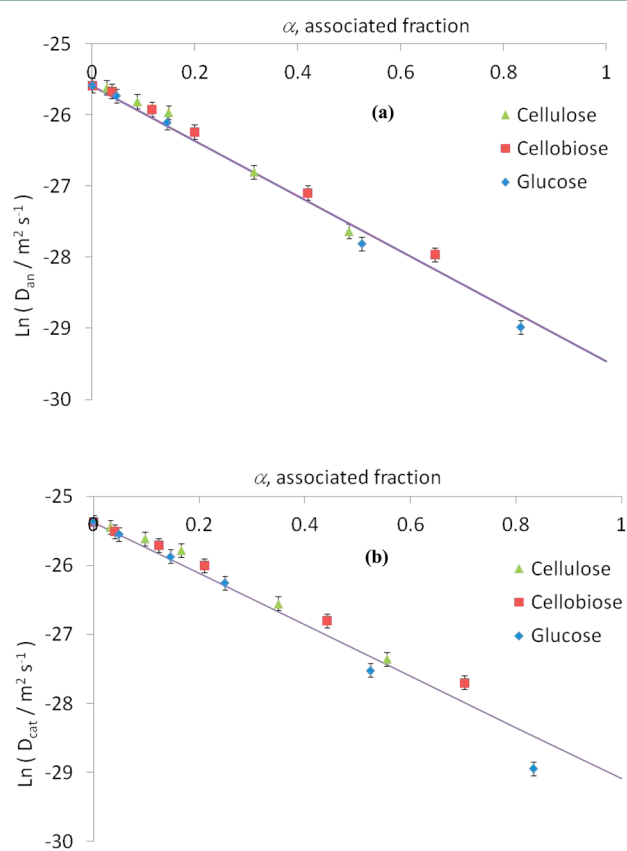


**Figure 5.** Diffusion coefficients of the anion  $D_{an}$  (a) and cation  $D_{cat}$  (b) at 20 °C as a function of associated fraction  $\alpha$  as defined by eq 2, taking  $N$  to be 5:4:3 for glucose/cellobiose/cellulose, respectively. The solid lines are linear fits to the data.

In Figure 5a it can be seen that the data collapse onto a master curve when plotted as a function of associated fraction  $\alpha$ . The diffusion coefficient of the anion is therefore predominantly determined by the number of OH groups of the solute that the ionic liquid has to satisfy. It is important to observe that the curvature seen in Figure 4a when plotting against weight fraction has been removed, with the data now being well described by a linear fit, see the solid line in Figure 5a. We put this forward as strong evidence that the parameter  $\alpha$  is the correct one to describe the effect of the carbohydrate solute on the microscopic translational mobility of the anions in these systems. What is interesting to discover, see Figure 5b, is that this same relationship holds almost as well for the cations.

The  $N$  used in Figure 5 were 5:4:3 for glucose/cellobiose/cellulose, but it is possible to vary these numbers (keeping one, here the cellulose  $N = 3$  value, fixed) to obtain the best overlap as determined by a least-squares fit. In this sense,  $N$  can then be thought of as the number of IL molecules associated per carbohydrate molecule. For the anion, the ratio becomes 5.2:3.7:3, and for the cation, the ratio becomes 6.0:3.8:3.0, with an uncertainty on all these values of  $\pm 0.4$ . It is worth mentioning that when these ratios are used instead of 5:4:3 all the data, when replotted, then lie on straight lines well within the experimental uncertainties, even improving on the quality of the fits shown in Figure 5, with the most notable improvement being to the cation glucose data. This suggests therefore that more cations than anions are associated per glucose molecule. This is consistent with a molecular dynamics study of glucose dissolved in [C2mim][OAc], where five anions were found around a glucose molecule and up to the same cutoff distance there were nearly six cations.<sup>24</sup>

It is often said that the anion plays the key role in dissolving the carbohydrate. Our data supports this, recall Figure 3, but in Figure 5 we see that the cation is similarly affected by the OH groups of the solute in terms of its translation mobility. This is quantified by the slopes of the straight lines in Figure 5, which measure the degree of reduction in diffusion coefficient per increase in the ratio of OH groups to IL molecules. The slopes in Figure 5 are  $-3.9 \pm 0.4$  and  $-3.7 \pm 0.4$  for the anion and cation, respectively, with them being of similar values given their uncertainties.

To explain the origin of the linear dependence of  $\ln D$  vs  $\alpha$  found in Figure 5 we consider the ions to be either associated to a carbohydrate molecule or free, with a fraction  $\alpha$  being in the associated state. Next we assume that there is fast exchange between the free and associated ions and that therefore the resultant activation energy of diffusional (translational) motion,  $E_A$  is given by

$$\begin{aligned} E_A &= (1 - \alpha)E_{free} + \alpha E_{associated} \\ &= \alpha(E_{associated} - E_{free}) + E_{free} \\ &= \alpha \Delta E + E_{free} \end{aligned} \quad (3)$$

where  $E_{free}$  is the translational activation energy of the free ions,  $E_{associated}$  that for the associated ions, and  $\Delta E = E_{associated} - E_{free}$  is the difference in activation energies between the associated and free states. The diffusion coefficient is given by

$$D = D_0 \exp\left(-\frac{E_A}{RT}\right) \quad (4)$$

with  $T$  being temperature and  $R$  being the universal gas constant. Note that the  $D_0$  and  $E_A$  will have different numerical values for the cation and anion. Substituting eq 3 into eq 4 and taking the natural logarithm gives

$$\ln D = \left(\ln D_0 - \frac{E_{free}}{RT}\right) - \alpha \times \frac{\Delta E}{RT} \quad (5)$$

The first term on the right-hand side of eq 5 in the brackets is a constant independent of  $\alpha$ . Equation 5 therefore predicts a linear dependence of  $\ln D$  on  $\alpha$ , which is consistent with the data in Figure 5.

It is interesting to note that eq 5 resembles the ideal mixing law approach for diffusion<sup>34</sup> when interpreted in terms of a "mixture" of free and associated ions. Eq 5 can be rewritten as

$$\ln(D) = (1 - \alpha) \ln D_{\text{free}} + \alpha \ln D_{\text{associated}} \quad (6)$$

where  $(1 - \alpha)$  is the mole fraction of free ions,  $D_{\text{free}}$  is the diffusion coefficient for these free ions,  $\alpha$  is the mole fraction of associated ions, and  $D_{\text{associated}}$  is the diffusion coefficient for these associated ions. In this likening

$$D_{\text{free}} = D_0 \exp\left(-\frac{E_{\text{free}}}{RT}\right) \quad (7)$$

and

$$D_{\text{associated}} = D_0 \exp\left(-\frac{E_{\text{associated}}}{RT}\right) \quad (8)$$

From Figure 5 and eq 5 we can determine  $\Delta E$ , as this is given by the slope of the straight line fits. This produces a value of  $9.3 \pm 0.9$  kJ/mol to the difference in activation energy between the associated and the free ions, with this being approximately the same value for both the cation and the anion within the uncertainty given. Next, by considering the temperature dependence of our data this numerical value for  $\Delta E$ , determined above purely from the concentration analysis, can be independently verified, and in doing this, we will also be able to check our starting assumption, eq 3.

To determine  $\Delta E$ , the temperature dependence of the anion and cation diffusion coefficients in the carbohydrate solutions will be fitted using an Arrhenius approach, see eq 4. For each concentration and each carbohydrate system, an activation energy will be found from a least-squares analysis. The value of  $D_0$  across all the samples will be treated as a global fitting parameter in the sense that there will only be one  $D_0$  for all the cation data in all the carbohydrate solutions and similarly one  $D_0$  for all the anion data. In this way the analysis is a more rigorous test of the Arrhenius behavior and  $D_0$  represents a fundamental property of each ion itself. Furthermore, if it is possible to obtain satisfactory fits with this extra constraint then this indicates that allowing  $D_0$  to vary would not generate any extra meaningful information.

A selection of the temperature dependences of cation diffusion with the corresponding fits of eq 4 is shown in Figure 6. A similar quality of fit was obtained for all the other data, including the anion results.

In Figure 6 it can be seen that the data reasonably follow an Arrhenius behavior. The same analysis was carried out for the anion diffusion in glucose, cellobiose and cellulose solutions.

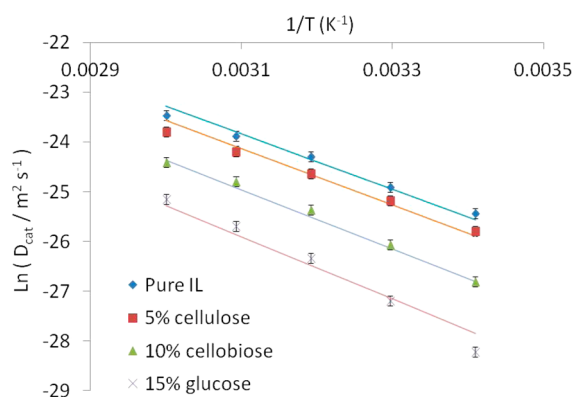


**Figure 6.** Examples of diffusion coefficient of the cation  $D_{\text{cat}}$  in glucose, cellobiose, and cellulose solutions as a function of inverse temperature. The solid lines are fits to eq 4.

The value of  $D_0$  for the anion data is  $1.6 \pm 0.2$  m<sup>2</sup> s<sup>-1</sup> ( $D_{0,\text{an}}$ ) and for the cation data is  $1.4 \pm 0.2$  m<sup>2</sup> s<sup>-1</sup> ( $D_{0,\text{cat}}$ ). It is interesting to notice that the  $D_0$  values for the cation and anion are not “anomalous” ( $D_{0,\text{an}}/D_{0,\text{cat}} = 1.14 > 1$ ), unlike the diffusion coefficients themselves in these systems ( $D_{\text{an}}/D_{\text{cat}} < 1$ , see Figure 3). By this we mean that  $D_0$  for the cation is smaller than  $D_0$  for the anion consistent with the relative sizes of the ions. The diffusion coefficients  $D$  tend to  $D_0$  as  $E_A$  tends to zero, that is, when all the interactions of the ions with their surroundings are removed. This reveals that the anomalous behavior is due to the interactions of the ions with their environment, this being quantified through their activation energy terms.

In Figure 7a the anion activation energy found from the above analysis is shown as a function of carbohydrate associated

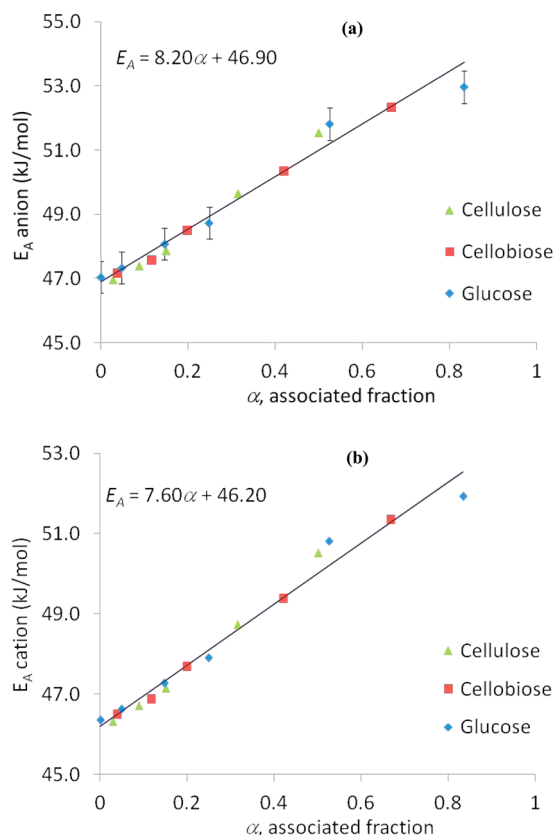


**Figure 7.** Anion (a) and cation (b) diffusion activation energy as a function of associated fraction  $\alpha$  as defined by eq 2. The solid lines are a linear fit to the data. The size of the uncertainties is shown for the glucose anion data and each series has a similar sized uncertainty, which has been left off the figure for clarity.

fraction  $\alpha$ , the same for the cation is presented in Figure 7b. Both figures show that the activation energies for cation and anion are, to a very good approximation, linear in  $\alpha$ , consistent with eq 3. This strengthens the hypothesis that it is the ratio of OH groups to ionic liquid molecules that determines the diffusional dynamics in these carbohydrate–ionic liquid solutions.

The slopes of  $E_A$  versus  $\alpha$  for the anion (Figure 7a) and for the cation (Figure 7b) give us directly the difference between the activation energy  $\Delta E$  of the associated ions ( $\alpha = 1$ ) and the free ions ( $\alpha = 0$ ). Therefore,  $\Delta E$  is  $8.2 \pm 0.4$  kJ/mol for the anion and  $7.6 \pm 0.4$  kJ/mol for the cation. These values, which

have been independently determined from examining the temperature dependence of the diffusion data, match reasonably well with the value of  $\Delta E = 9.3 \pm 0.9$  kJ/mol found earlier from examining the concentration dependence in Figure 5 by eq 5.

**$^1\text{H}$  NMR Spectra: Chemical Shifts as a Function of Carbohydrate Concentration.** We now turn to the proton spectra from our samples and examine how the positions of the resonance peaks change upon addition of carbohydrate. For each solution of our [C2mim][OAc] and carbohydrate proton spectra were measured at 20 to 70 °C. The assigned proton resonances (1–7) for the [C2mim][OAc] molecule are shown in Figure 8. In our work, proton resonance 5 was used as a

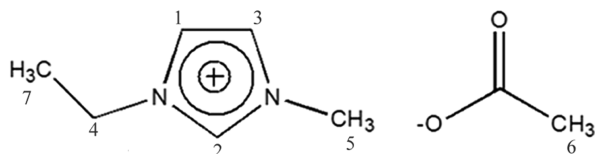


**Figure 8.** Chemical structure of [C2MIM]<sup>+</sup> and [OAc]<sup>−</sup> ions of 1-ethyl-3-methyl-imidazolium acetate with the proton resonances (1–7) labeled.

reference point; we determined the chemical shift  $\delta$  of all the other resonances via their distances from this peak. This method follows several other  $^1\text{H}$  NMR studies on imidazolium based ILs where the chemical shift of the methyl group (peak 5) has been shown to be largely independent of extrinsic variables, such as IL concentration in water/1-alkyl-3-methylimidazolium bromide solutions<sup>35</sup> and cellobiose concentration<sup>17</sup> upon solvation in [C2mim][OAc]. Finally, we do not have any unassigned peaks and the proportion of anion signal is correct for all our samples, and therefore, the amount of acetylation of our carbohydrates, if any, must be small <5% (w/w).<sup>6,36</sup>

To calculate the change in position of the peaks  $\Delta\delta$  on the addition of a carbohydrate, we used the  $\delta$  for each resonance in the pure ionic liquid sample as a starting reference value, so that  $\Delta\delta$  corresponds to the change in parts per million (ppm) of a peak from that of the pure [C2mim][OAc]. In Figure 9 the change in peak position  $\Delta\delta$  is plotted as a function of weight percentage of glucose.

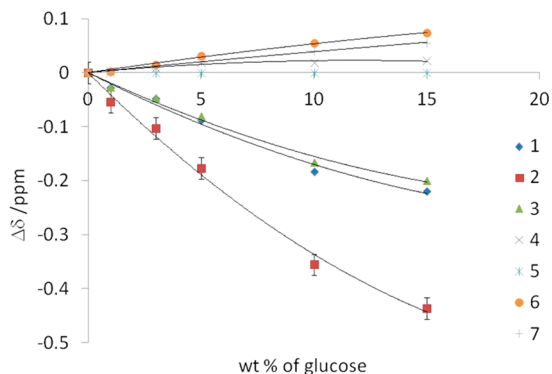


**Figure 9.**  $\Delta\delta$  at 40 °C vs weight fraction of glucose for the various [C2mim][OAc] resonances (1–7), recall Figure 8. The lines are guides to the eye. The size of the uncertainties is shown for the peak 2 data and each peak has similar sized uncertainty, which has been left off the figure for clarity.

Peak 2 shows the most movement in its resonance position upon the addition of glucose, with this being the most acidic proton on the imidazolium ring. All the ring protons (1–3) have negative values for their  $\Delta\delta$ s, with this corresponding to an upfield movement and indicates that the addition of glucose has disrupted strong ion associations in the pure [C2mim][OAc] via additional H-bonding with the OH groups on the sugar. This displacement is consistent with the acetate anion preferentially forming hydrogen bonds with the glucose molecules and therefore on the addition of glucose leaving the ring protons of the cation, causing their upfield shift. Peak 4, the  $\text{CH}_2$  group in the alkyl chain, is hardly affected by the addition of glucose, which is similar to that observed in previous work.<sup>35</sup> Peaks 6 and 7, the two methyl groups, have a small downfield shift, with this being observed before upon the addition of cellobiose<sup>17</sup> and cellulose.<sup>22</sup>

In Figure 10 the  $\Delta\delta$  for the selected peaks 2, 3, and 6 are shown for the cellulose, cellobiose, and glucose data all

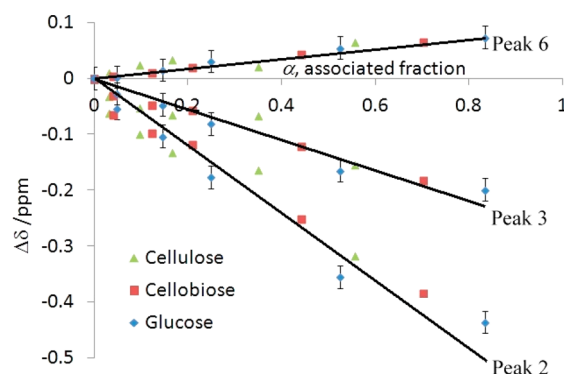


**Figure 10.**  $\Delta\delta$  for cellulose, cellobiose, and glucose at 40 °C vs associated fraction  $\alpha$ , as defined by eq 2 for the various [C2mim][OAc] resonances 2, 3, and 6, recall Figure 8. The lines are guides to the eye. The size of the uncertainties is shown for the glucose data and each series has a similar sized uncertainty, which has been left off the figure for clarity.

combined together but now plotted as a function of  $\alpha$ , the associated fraction. These peaks now each fall onto their own master curve. This result is also true for the other resonances not shown in Figure 10. This reveals that not only are the translational dynamics being determined by the ratio of OH groups to IL molecules, but so are the chemical environments of all the hydrogen nuclei. This is an independent confirmation of the hypothesis that the key parameter in understanding these systems is therefore the associated fraction  $\alpha$ , defined by eq 2.

## CONCLUSIONS

In this work we have analyzed the NMR determined diffusion coefficients, across the temperature range 20–70 °C, of the ions in pure [C2mim][OAc] and three sets of samples (glucose/cellobiose/cellulose), each with five concentrations of the carbohydrate (1, 3, 5, 10, and 15% w/w) dissolved in [C2mim][OAc]. Across all our measurements, each NMR proton resonance displayed only one diffusion coefficient, indicating that if ion pairs or aggregates are forming then there must be fast exchange between the free ions and the pairs and aggregates. For all our samples, an increase in temperature was found to increase the diffusion coefficients, whereas an increase of the carbohydrate concentration decreased them.

As in other published work<sup>29</sup> on the diffusion of ions in [C2mim][OAc], we likewise found that the anion, though geometrically smaller than the cation, diffuses slower than its counterion, this being so for the cellulose, cellobiose, and glucose solutions. On the addition of carbohydrate, this “anomalous” diffusion became more pronounced with the ratio  $D_{\text{an}}/D_{\text{cat}}$  reducing yet further. We explained this in terms of the anion being more directly involved in the dissolution of the carbohydrates, with these interactions preferably slowing down the motion of the anions relative to the cations. Glucose was the most effective molecule at reducing this ratio of the diffusion coefficients and cellulose the least effective for any given weight concentration.

We demonstrated that glucose, weight for weight, reduced the diffusion coefficients of the ions the most from that of their pure IL values. Conversely, cellulose reduced them the least. In terms of a Stokes–Einstein analysis, the ions in the glucose system therefore experience the highest effective local level microviscosity, for a given concentration of carbohydrate. This result is at odds with the macroscopic properties of these solutions in that it is the cellulose samples that have the highest zero shear rate viscosities.

To explain this result we introduced the parameter  $\alpha$ , which is equal to the molar ratio of OH groups on the carbohydrate molecules (glucose/cellobiose/cellulose) to [C2mim][OAc] molecules. All the diffusion coefficients for each ion in cellulose, cellobiose, and glucose solutions then fell onto a master curve when plotted against this term. From this analysis we determined the number  $N$  of [C2mim][OAc] molecules associated with a carbohydrate molecule. For the anion we found 5.2:3.7:3.0 for glucose/cellobiose/cellulose and for the cation 6.0:3.8:3.0. This indicates that more cations are associated per glucose molecule than anions, with this agreeing with a recent computer simulation.<sup>24</sup> The linear dependencies of the logarithm of diffusion coefficient as a function of  $\alpha$  were then explained in terms of an “ideal mixing”<sup>34</sup> of free ions and ions that are associated with carbohydrate molecules. The difference in activation energies for the translational diffusional motion of the associated and free ions is  $9.3 \pm 0.9$  kJ/mol, this being the same value for both the cation and the anion within the stated uncertainty. It should be noted that this value was determined without varying the temperature and found from purely analyzing the concentration dependence.

All the diffusion data have Arrhenius temperature dependence. The prefactor  $D_0$  in the Arrhenius diffusion expression, found from fitting our data, gave a value for the anion equal to  $1.6 \pm 0.2$  m<sup>2</sup> s<sup>-1</sup> and for the cation  $1.4 \pm 0.2$  m<sup>2</sup> s<sup>-1</sup>. Here  $D_{0,\text{anion}} > D_{0,\text{cation}}$  and therefore the “anomalous” diffusion found in [C2mim][OAc] and its solutions is due to the interactions of the ions with their environment. For each ion, the activation energy was found to have a linear dependence on  $\alpha$ , confirming our assumption of the ideal mixing of free and associated ions. The difference in activation energies of the free and associated ions is equal to  $8.2 \pm 0.4$  kJ/mol for the anions and  $7.6 \pm 0.4$  kJ/mol for the cations. These values determined from the temperature dependence agreed well with the value found independently from the concentration analysis.

The changes in ppm  $\Delta\delta$  of the various [C2mim][OAc] proton resonances due to the presence of dissolved carbohydrate were studied. The movement of the various peaks was consistent with the acetate ions preferentially forming hydrogen bonds with the carbohydrate molecules. Finally, when  $\Delta\delta$  were plotted as a function of  $\alpha$  each

resonance peak for the cellulose, cellobiose, and glucose solutions all collapsed together onto their own corresponding master curves. This showed that not only is the diffusion of the ions being determined by the molar ratio of OH groups to [C2mim][OAc] molecules, but so also are the chemical environments of each hydrogen in the ionic liquid.

## AUTHOR INFORMATION

### Corresponding Author

\*E-mail: m.e.ries@leeds.ac.uk

### Notes

The authors declare no competing financial interest.

## ACKNOWLEDGMENTS

M.E.R. is a Royal Society Industry Fellow. The authors are grateful for the EPSRC seed money EP/1500286/1. A.R. is funded by the Malaysian Government.

## REFERENCES

- (1) Wang, H.; Gurau, G.; Rogers, R. D. *Chem. Soc. Rev.* **2012**, *41* (4), 1519–1537.
- (2) Klemm, D.; Heublein, B.; Fink, H. P.; Bohn, A. *Angew. Chem., Int. Ed.* **2005**, *44* (22), 3358–3393.
- (3) Swatloski, R. P.; Spear, S. K.; Holbrey, J. D.; Rogers, R. D. *J. Am. Chem. Soc.* **2002**, *124* (18), 4974–4975.
- (4) Ohno, H.; Fukaya, Y. *Chem. Lett.* **2009**, *38* (1), 2–7.
- (5) Angell, C. A.; Ansari, Y.; Zhao, Z. F. *Faraday Discuss.* **2012**, *154*, 9–27.
- (6) Karatzos, S. K.; Edey, L. A.; Wellard, R. M. *Cellulose* **2012**, *19* (1), 307–312.
- (7) Fort, D. A.; Remsing, R. C.; Swatloski, R. P.; Moyna, P.; Moyna, G.; Rogers, R. D. *Green Chem.* **2007**, *9* (1), 63–69.
- (8) Brandt, A.; Grasvik, J.; Hallett, J. P.; Welton, T. *Green Chem.* **2013**, *15* (3), 550–583.
- (9) Bose, S.; Armstrong, D. W.; Petrich, J. W. *J. Phys. Chem. B* **2010**, *114* (24), 8221–8227.
- (10) Hou, J. B.; Zhang, Z. Y.; Madsen, L. A. *J. Phys. Chem. B* **2011**, *115* (16), 4576–4582.
- (11) Sowmiah, S.; Srinivasadesikan, V.; Tseng, M. C.; Chu, Y. H. *Molecules* **2009**, *14* (9), 3780–3813.
- (12) Kosan, B.; Michels, C.; Meister, F. *Cellulose* **2008**, *15* (1), 59–66.
- (13) Cao, Y.; Li, H. Q.; Zhang, Y.; Zhang, J.; He, J. S. *J. Appl. Polym. Sci.* **2010**, *116* (1), 547–554.
- (14) Sescousse, R.; Gavillon, R.; Budtova, T. *Carbohydr. Polym.* **2011**, *83* (4), 1766–1774.
- (15) El Seoud, O. A.; Koschella, A.; Fidale, L. C.; Dorn, S.; Heinze, T. *Biomacromolecules* **2007**, *8* (9), 2629–2647.
- (16) Remsing, R. C.; Swatloski, R. P.; Rogers, R. D.; Moyna, G. *Chem. Commun.* **2006**, *12*, 1271–1273.
- (17) Zhang, J. M.; Zhang, H.; Wu, J.; Zhang, J.; He, J. S.; Xiang, J. F. *Phys. Chem. Chem. Phys.* **2010**, *12* (8), 1941–1947.
- (18) Liu, H. B.; Sale, K. L.; Holmes, B. M.; Simmons, B. A.; Singh, S. *J. Phys. Chem. B* **2010**, *114* (12), 4293–4301.
- (19) Gericke, M.; Schlufter, K.; Liebert, T.; Heinze, T.; Budtova, T. *Biomacromolecules* **2009**, *10* (5), 1188–1194.
- (20) Haward, S. J.; Sharma, V.; Butts, C. P.; McKinley, G. H.; Rahatekar, S. S. *Biomacromolecules* **2012**, *13* (5), 1688–1699.
- (21) Kuang, Q. L.; Zhao, J. C.; Niu, Y. H.; Zhang, J.; Wang, Z. G. *J. Phys. Chem. B* **2008**, *112* (33), 10234–10240.
- (22) Lovell, C. S.; Walker, A.; Damion, R. A.; Radhi, A.; Tanner, S. F.; Budtova, T.; Ries, M. E. *Biomacromolecules* **2010**, *11* (11), 2927–2935.
- (23) Remsing, R. C.; Hernandez, G.; Swatloski, R. P.; Masefski, W. W.; Rogers, R. D.; Moyna, G. *J. Phys. Chem. B* **2008**, *112* (35), 11071–11078.



- (24) Youngs, T. G. A.; Holbrey, J. D.; Mullan, C. L.; Norman, S. E.; Lagunas, M. C.; D'Agostino, C.; Mantle, M. D.; Gladden, L. F.; Bowron, D. T.; Hardacre, C. *Chem. Sci.* **2011**, *2* (8), 1594–1605.
- (25) Rabideau, B. D.; Agarwal, A.; Ismail, A. E. *J. Phys. Chem. B* **2013**, *117* (13), 3469–3479.
- (26) Holz, M.; Heil, S. R.; Sacco, A. *Phys. Chem. Chem. Phys.* **2000**, *2* (20), 4740–4742.
- (27) Annat, G.; MacFarlane, D. R.; Forsyth, M. *J. Phys. Chem. B* **2007**, *111* (30), 9018–9024.
- (28) Cotts, R. M.; Hoch, M. J. R.; Sun, T.; Markett, J. T. *J. Magn. Reson.* **1989**, *83*, 252–266.
- (29) Menjoge, A.; Dixon, J.; Brennecke, J. F.; Maginn, E. J.; Vasenkov, S. *J. Phys. Chem. B* **2009**, *113* (18), 6353–6359.
- (30) Noda, A.; Hayamizu, K.; Watanabe, M. *J. Phys. Chem. B* **2001**, *105* (20), 4603–4610.
- (31) Tokuda, H.; Hayamizu, K.; Ishii, K.; Abu Bin Hasan Susan, M.; Watanabe, M. *J. Phys. Chem. B* **2004**, *108* (42), 16593–16600.
- (32) Tokuda, H.; Hayamizu, K.; Ishii, K.; Susan, M.; Watanabe, M. *J. Phys. Chem. B* **2005**, *109* (13), 6103–6110.
- (33) Tokuda, H.; Ishii, K.; Susan, M.; Tsuzuki, S.; Hayamizu, K.; Watanabe, M. *J. Phys. Chem. B* **2006**, *110* (6), 2833–2839.
- (34) Hall, C. A.; Le, K. A.; Rudaz, C.; Radhi, A.; Lovell, C. S.; Damion, R. A.; Budtova, T.; Ries, M. E. *J. Phys. Chem. B* **2012**, *116* (42), 12810–12818.
- (35) Zhao, Y.; Gao, S. J.; Wang, J. J.; Tang, J. M. *J. Phys. Chem. B* **2008**, *112* (7), 2031–2039.
- (36) Ebner, G.; Schiehser, S.; Potthast, A.; Rosenau, T. *Tetrahedron Lett.* **2008**, *49* (51), 7322–7324.